

David supports Goliath: Investigating the role of Zwint-1 in kinetochore assembly mediated by KNL1

Tim van der Plas

RESEARCH REPORT MAJOR INTERNSHIP

Supervisor: Jingchao Wu

Examiner: Geert Kops

Kops group – Hubrecht institute

January 4th 2021

Layman's summary

In order to sustain the tissues of the human body, cells need to divide constantly. This division process, named mitosis, requires equal separation of our genetic material from the mother cell to two daughter cells. In order to equally separate, our DNA is duplicated during an earlier moment of the cell's life cycle. During mitosis, our DNA will congress into chromosomes which allow for the DNA to be moved around the cell. These chromosomes will find their duplicated pair, and align in a neat plate in the middle of the cell, after which microtubules, the cytoskeletal cables of the cell, attempt to attach on both sides of the chromosome pairs. This attachment requires an intricate protein complex to mediate interactions between the microtubule and the chromosome. This protein complex is called the kinetochore, and it consists of many different proteins that each carry out their own important function. It is important that the kinetochore mediates this attachment thoroughly. The chromosome pairs need to segregate from each other, and for every pair, each chromosome needs to end up in a different daughter cell. That way, both daughter cells acquire the same chromosomes, and our DNA content stays intact. If segregation defects were to occur, daughter cells could end up with unequally distributed DNA contents, which cause many problems for the cell and often result in cell death. To regulate microtubule attachment, the kinetochore assembles, interacts with the microtubule, and checks whether stable attachment has been established. If so, it will signal to the cell that mitosis can continue. An important protein within the kinetochore structure is KNL1. KNL1 has a large and unstructured shape, which functions as a scaffold for other proteins to interact with. If KNL1 is prohibited from forming in experiments, the kinetochore structure gets disturbed and many proteins fail to localize to their normal spot in the kinetochore. This disturbed kinetochore has difficulty carrying out its checking function, and chromosome segregation defects occur.

Here, the role of Zwint-1 in the kinetochore is investigated. Zwint-1 has a close interaction with KNL1, even though it is more than eight times smaller in size. Through genetic modification, the Zwint-1 protein can be 'knocked out' of the cell, creating a cell line that tries to live even though there is no Zwint-1 protein available. This Zwint-1 knockout displays a disturbed kinetochore that looks similar to how the kinetochore is disturbed when KNL1 is taken away. Additionally, the disturbed kinetochore resulting from the Zwint-1 knockout exhibits increasing amounts of chromosome segregation defects and mitosis duration is decreased. This indicates that the cell might have trouble correctly signalling for proper microtubule attachment to the kinetochore. When Zwint-1 is introduced back into the cell line, the kinetochore forms more similar to how it should, and the segregation defects disappear. Taken together, Zwint-1 appears to have a significant role in the structure of the kinetochore. Given its size and localization, it is hypothesized that Zwint-1 could have a supporting role for the large KNL1 protein, making sure that it can stably scaffold the kinetochore structure. More research on the precise mechanisms of interaction between KNL1 and Zwint-1 could further confirm this hypothesis.

Abstract

Proper assembly of the kinetochore is essential for correct microtubule attachment and stable chromosome segregation during mitosis. KNL1 is a large scaffolding protein central to formation of the kinetochore which initiates spindle assembly checkpoint signalling to halt anaphase onset until microtubule attachment has been established. Given its important role in ensuring stable chromosome segregation, functioning of KNL1's recruiters and close interactors Zwint-1 and Mis12 should also be acknowledged. Here, the role of Zwint-1 in the kinetochore is addressed, as previous research hasn't been able to robustly identify the function of Zwint-1. A Zwint-1 knockout RPE1 cell line is presented, which exhibits increased chromosome segregation defects and a decreased time in mitosis. Immunofluorescence assessment of the kinetochore structure reveals disturbed localization of many kinetochore proteins, namely Bub1 and BubR1, as well as fibrous corona proteins CENP-E and Mad1. Furthermore, interkinetochore distance was increased in the Zwint-1 KO line, and formation of fibrous corona structures is impaired. Expressing Zwint-1 rescue constructs in the knockout line restores both localization of the outer kinetochore proteins and chromosome segregation integrity. These findings illustrate the relevance of Zwint-1 in the kinetochore, and warrant further research in the precise mechanics behind its interaction with KNL1 to stabilize the kinetochore structure.

Introduction

Cell division in eukaryotes requires equal separation of the replicated genome from a mother cell to its daughters. In mitosis, microtubules bind to all sister chromatids of the cell and initiate equal distribution into both daughter cells. In humans, this is an intricate and highly regulated process, as unequal distribution of genetic material can lead to a plethora of problems [1]. In order to properly regulate this process of chromatid separation, a large multi-subunit protein complex, the kinetochore, is assembled [2,3]. The kinetochore is the site on the chromatid that establishes the connection with the microtubules of the mitotic spindle. When all chromatids are connected with the spindle microtubules, separation of the sister chromatids is initiated.

Assembly of the kinetochore

The kinetochore structure is constructed at a specific locus on the chromatin, called the centromere, and can be divided into two sections: the inner kinetochore and the outer kinetochore [4,5]. Incorporation of the H3 histone variant centromeric protein A (CENP-A) decides on the location of the centromere. The location of CENP-A incorporation is defined epigenetically, and this centromeric chromatin forms the base for kinetochore formation. CENP-A is then recognized by other centromeric proteins (CENP), namely CENP-C and CENP-N [6]. This is but the start of the formation of the constitutive centromere-associated network (CCAN; also known as the interphase centromere complex (ICEN)). The CCAN is a network of 16 CENPs that recognize the centromeric histone and form the centre of the inner kinetochore [7].

In addition to the inner kinetochore, the outer kinetochore is the site where interaction with the microtubules is established. The centre of this outer kinetochore is a network of 10 proteins known as the KMN (KNL1 complex, Mis12 complex, Ndc80 complex) network [8,9,10]. The Mis12 complex is the hub that constitutes KMN assembly by interacting with both the Ndc80 complex and KNL1 complex. By doing so, Mis12 can connect these complexes to the inner kinetochore, as it also binds to inner kinetochore proteins CENP-C and CENP-T [11,12,13]. The Ndc80 complex is the main interactor for the kinetochore with the ends of microtubules, and therefore establishes the contact between the kinetochore and the mitotic spindle. Still much research is devoted to uncovering the details of the mechanism behind this interaction [14,15]. KNL1 is the largest of the outer kinetochore subunits. N-terminally, KNL1 contains a large disordered residue chain which carries an array of Met-Glu-Leu-Thr (MELT) repeats, which act as docking sites for the Spindle Assembly Checkpoint (SAC, also known as mitotic or metaphase checkpoint) [16,17].

The Spindle Assembly Checkpoint

The SAC is a control mechanism that will halt mitosis until all chromosomes are correctly bi-orientated and attached to microtubules of the mitotic spindle [18,19]. Therefore, the SAC will prevent premature chromosome segregation, and in doing so, it safeguards proper distribution of the genome into the daughter cells. In order to carry out this function, the SAC must inhibit the anaphase-promoting

complex or cyclosome (APC/C) E3 ubiquitin ligase, whose main function is to promote anaphase. The APC/C is activated via phosphorylation by cyclin-dependent kinases (Cdks), and can then activate its substrates cyclin B and securin for polyubiquitination followed by degradation by the proteasome. Destruction of these substrates starts anaphase, as sister chromosome pairs are separated and distribution of chromosomes is conducted. A key cofactor for the ubiquitin activity of APC/C is Cell-division cycle protein 20 homologue (Cdc20). The SAC targets and inhibits Cdc20, and by doing so prevents activation of the APC/C [20]. Altogether, this intricate pathway holds mitosis in check until proper end-on attachment of microtubules to the kinetochore is formed. Proper functioning of the SAC is paramount to genomic integrity in cells. However, as explained above, the SAC pathway requires a fascinating orchestra of proteins to dynamically localize to and from the kinetochore [21]. Many alterations in the kinetochore lead to defects in SAC signalling, causing premature chromosome segregation, often associated with aneuploidy resulting in apoptosis [66].

KNL1 as scaffold for assembly of the kinetochore and recruitment of the Fibrous Corona

One of the main and initial players in the SAC pathway is KNL1 (also known as CASC5, AF15Q14 and Blinkin). As the largest outer kinetochore protein, KNL1 functions as an important scaffold protein and was shown to play a role in kinetochore assembly and chromosome congression, aside from the described role in SAC signalling [22]. It predominantly has an intrinsically disordered structure, with only the last ~500 of its 2316 residues containing a determined structure. The predetermined C-terminal structure of KNL1 forms a coiled coil and several RWD domains. This structure establishes a direct interaction with Mis12, and additionally creates a binding domain for Zeste White 10 (ZW10) interactor 1 (Zwint-1) [23]. The large and unstructured side of KNL1 contains 19 MELT-like motifs that form the base for recruitment of the MCC. Monopolar spindle 1 (Mps1) kinase, which is recruited to the kinetochore via Ndc80 in early prophase, targets these MELT motifs [24]. The Mps1-dependent phosphorylation of the threonine in the MELT sites on KNL1 recruits a complex of budding uninhibited by benzimidazoles 1 (Bub1) and budding uninhibited by benzimidazole 3 (Bub3) [25,26,27,28,29,30,31,32]. The Bub1-Bub3 complex in turn recruits a complex of Bub3 with the budding uninhibited by benzimidazoles related 1 (BubR1), accompanied by a complex of mitotic arrest deficient 1 and 2 (Mad1-Mad2) [33,34,35]. Mad2 is then transformed from an inactive and open conformation to an active and closed conformation, which favours interaction and subsequent inhibition of APC/C cofactor Cdc20 [36]. It was shown how these MELT motifs have an additive effect for recruiting the Bub proteins [37]. Interestingly, only 4 of the 19 MELT-like motifs on the KNL1 scaffold are needed to establish the function of KNL1 in chromosome congression and SAC protein recruitment [38]. Additionally, the MELT motifs on KNL1 contain flanking KI motifs which are not essential for SAC recruitment, but do stabilize interactions with the Bub proteins [39]. KNL1 depletion delocalizes many of the other downstream kinetochore proteins, ranging from the MCC subunits to the fibrous corona subunits such as the RZZ complex [56,57,58]. This further indicates the scaffolding role of KNL1, and the precise mechanisms of interaction are an active field of research.

As stated before, the KMN network needs to establish this connection of the kinetochore with the microtubules of the spindle. It is thought that in order to increase the likelihood of microtubule capture, the outer kinetochore expands into a crescent-like surface consisting of several proteins [40,41]. This expanded structure was named the fibrous corona, reflecting its crescent- or crown like structure around the kinetochore. Known protein complexes that form the fibrous corona include microtubule motors (CENP-E, dynein), microtubule associated proteins (MAPs), SAC proteins, and the Rod-Zwilch-ZW10 (RZZ) complex [42,43,44,45,46,47]. The RZZ complex recruits Dynein (a minus-end directed microtubule motor) [48]. Upon end-on kinetochore attachment mediated by Ndc80, the fibrous corona structure changes to a plate-like appearance, initiating the release of the Dynein-Dynactin-Spindly-RZZ complex, which will move towards the spindle poles due to the motor activity of Dynein. The Mad1-Mad2 complex, a part of the SAC, is also removed from the kinetochore via this mechanism [49,50,51]. As stated before, the Mad1-Mad2 complex inhibits Cdc20 from interacting with the APC/C to promote anaphase onset. When Mad1-Mad2 is moved towards the spindle poles, Cdc20 is released and together with an activated APC/C ubiquitinates cyclin B and securin to start anaphase and continue mitotic progression [52].

Current insights on Zwint-1 in the kinetochore

In this study, the role of Zwint-1 in the kinetochore structure is further assessed. Zeste White 10 Homolog (ZW10) interactor 1 (Zwint-1) was initially identified as the recruiter of ZW10 to the kinetochore, hence its name [53,54]. However, a few years later, it was shown how ZW10 mutants that fail to bind to Zwint-1 could still (less stably) localize to kinetochores [55]. More recently, it was shown how RZZ recruitment to the kinetochore depends on Bub1 instead of Zwint-1 [56]. Zwint-1 localizes to the kinetochore in prophase and remains there until anaphase. This localization is stable, as FRAP experiments showed how recovery of Zwint-1 after kinetochore bleaching is lacking [57].

The kinetochore localization domain of Zwint-1 is found at the N-terminus of the protein, while the C-terminus contains an interaction domain for ZW10. The latter site is found in the second of two coiled coil domains, both of which were found to be involved in Hec1 (a part of the Ndc80 complex) and ZW10 interactions [58]. Furthermore, Zwint-1 was shown to contain three phosphorylation sites C-terminally, which are targeted by the Aurora B kinase [59]. Zwint-1 degradation was shown to be regulated by the APC/C-Cdc20 complex in HEK293T cells. Upon activation after SAC passage, the APC/C-Cdc20 complex recognizes the D-boxes (R x x L) on Zwint-1 and targets it for degradation via ubiquitination [60].

Many of these characteristics could identify Zwint-1 as a possible structural protein involved in assembly of the kinetochore. However, as Zwint-1 is such a relatively small protein, it could be more likely to be involved in assisting kinetochore assembly, most prominently due to its interaction with the very large KMN network subunit KNL1. Zwint-1 interacts with KNL1 via RWD repeats on the structured C-terminal side of KNL1 [61]. In fact, KNL1 is recruited to the kinetochore via binding to both Mis12 and Zwint-1, both interactions mediated by the RWD repeats. Zwint-1 RNAi depletion leads to ~60%

reduction of KNL1 localization to the kinetochore, while KNL1 depletion abrogates kinetochore localization of both Zwint-1 and Mis12, elucidating to a co-dependency of between these proteins for localization to the kinetochore [62]. The discrepancy in the role of Zwint-1 in the kinetochore makes it an interesting protein to take a closer look at.

Given the proposed co-dependency between Zwint-1 and KNL1 for their kinetochore localization, the function of Zwint-1 in regards to KNL1 could be a very significant part of the kinetochore machinery. Here, research is conducted to address the uncertainties regarding the role and significance of Zwint-1 in the kinetochore. The aim is to gain further understanding in whether Zwint-1 is important for kinetochore structure, and how that role manifests itself in the functioning of the kinetochore. Firstly, an RPE-1 line containing a Zwint-1 knockout is presented. While the effect of RNAi knockdown off Zwint-1 in human cells has been explored before, a human cell line with a full Zwint-1 knockout provides an interesting platform to study the role of Zwint-1 in the kinetochore. Interestingly, the Zwint-1 knockout line showed decreased mitosis duration and chromosome segregation defects. Immunofluorescence assays on the localization of the outer kinetochore proteins downstream of KNL1 are conducted to analyse the stability of the kinetochore in absence of Zwint-1. It was found how Zwint-1 knockout destabilizes the kinetochore, as many of the outer kinetochore proteins show decreased localization to the kinetochore. Additionally, the distance between kinetochores of sister chromatids increased under Zwint-1 knockout, and the formation of the fibrous corona was impaired, further illustrating the destabilizing nature of Zwint-1 absence. By expressing Zwint-1 rescue constructs in the knockout line, localization of outer kinetochore proteins could be restored, and chromosome segregation defects were prevented. These findings illustrate the undeniable relevance of Zwint-1 in the kinetochore, and warrant further research in the mechanics of its interaction with KNL1 to stabilize the kinetochore structure.

Results

Zwint-1 can be successfully mutated to prevent its localization to kinetochore

In order to assess the role of Zwint-1 in the kinetochore, a solid model needed to be established. Therefore, a Zwint-1 mutant RPE1 cell line was created by introducing a mutation on the codon of the 60th amino acid of the WT Zwint-1 sequence, creating a stop codon after the 59th amino acid. In this model, the 1-59aa Zwint-1 mutant is expressed at less than 6% the value when compared to WT expression of Zwint-1, as analysed by qPCR (data not shown). In order to assess behaviour of the kinetochore in RPE1 cells, two inhibitors can be used to set the kinetochores to a specific state. Firstly, MG132, a proteasome inhibitor, inhibits degradation of targets ubiquitinated by APC/C [63]. As a result, while microtubule capture and attachment can occur uninterrupted, the spindle checkpoint cannot be overcome, and cells will arrest in metaphase. Chromosomes will remain on the metaphase plate, and the kinetochores can be analysed as being in an attached state. On the other hand, microtubule inhibitor Nocodazole (noco) can be used [64]. Noco will depolymerize β -tubulin, and therefore disrupt

spindle formation during mitosis. As no spindle microtubules will be formed, kinetochores will remain in an unattached state. Via immunofluorescence microscopy and by using CENP-C as a kinetochore marker, it can be seen how no WT Zwint-1 localizes to the kinetochore in MG132 treated cells (**Figure 1A**). Note that the specific primary antibody for Zwint-1 recognizes the C-terminal 55aa end of the protein, and therefore won't recognize the Zwint-1 1-59 mutant. By comparing the kinetochore localization of Zwint-1 in the mutant line to the signal from staining by solely the secondary antibody, therefore using no primary antibody for specific Zwint-1 targeting, it was confirmed that any very low signal of the Zwint-1 mutant line in the Zwint-1 channel was due to background signal caused by the fluorescent secondary antibody (**Figure 1A**, bottom row). The 1-59aa Zwint-1 mutant that is very lowly expressed will not localize to the kinetochore, as GFP-tagged constructs of Zwint-1 1-70 (data not shown) and 1-110 (**Figure 4**) do not localize to the kinetochore. Since this Zwint-1 mutant will not localize correctly to carry out its function in the kinetochore, this cell line will be referred to as Zwint-1 knockout (KO).

In order to quantify kinetochore localization, an analysis macro was written in the ImageJ software [65]. The macro looks for fluorescent signal colocalization between the protein of interest, in this case Zwint-1, and the kinetochore marker CENP-C. This colocalization level was normalized to wild-type (WT) and plotted to confirm the absence of kinetochore localization of Zwint-1 in the Zwint-1 KO line (**Figure 1B**, left part).

Additionally, both WT and Zwint-1 KO lines were treated with siRNA for Zwint-1 over 48 hours, to assess whether Zwint-1 knockdown could also achieve similar levels of Zwint-1 kinetochore depletion (**Figure 1B**, right part). While Zwint-1 knockdown affected Zwint-1 localization significantly, the Zwint-1 KO line gave the most robust Zwint-1 depletion. The imaging and analysis were also performed on Nocodazole (Noco) treated cells, and results were very similar, showing how in an unattached kinetochore state, Zwint-1 still does not localize in the mutant cell line (**Figure 1C, D**).

Zwint-1 knockout extends Mitosis duration and causes mitotic defects

An initial assessment of the Zwint-1 KO line was to look for changes in mitosis behaviour. Using live imaging fluorescent microscopy, duration of nuclear envelope breakdown (NEB) until anaphase onset was measured. By measuring this specific part of mitosis, it is possible to analyse whether the chromosomes have problems aligning to the metaphase plate, or whether the kinetochores have problems interacting with the microtubules of the mitotic spindle. Additionally, behaviour of the SAC can also be eluded from this analysis. In these experiments, it was found that while knockdown of Zwint-1 had no visible effect, Zwint-1 knockout did decrease NEB - anaphase duration significantly by ~10% (**Figure 2A**).

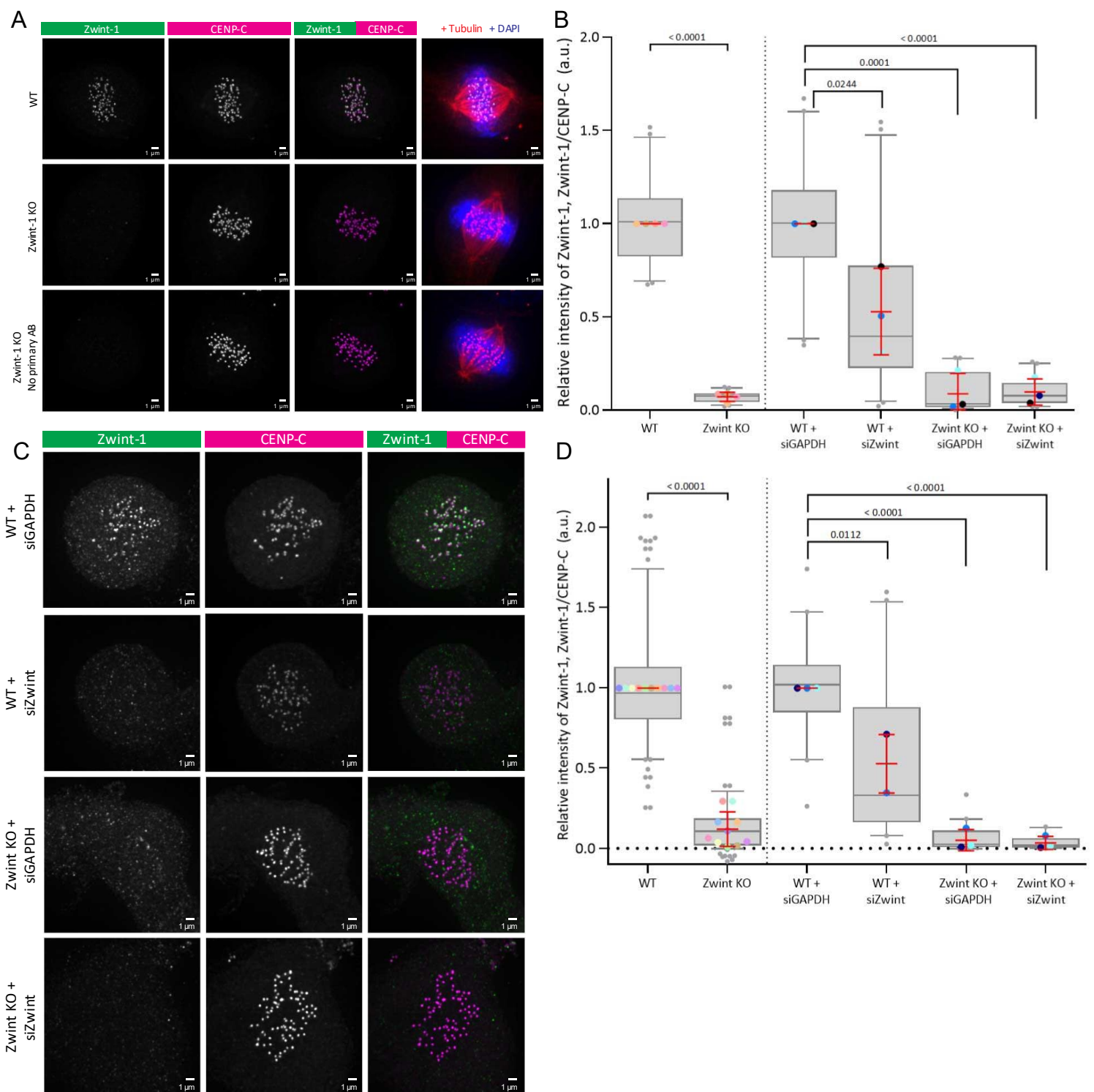
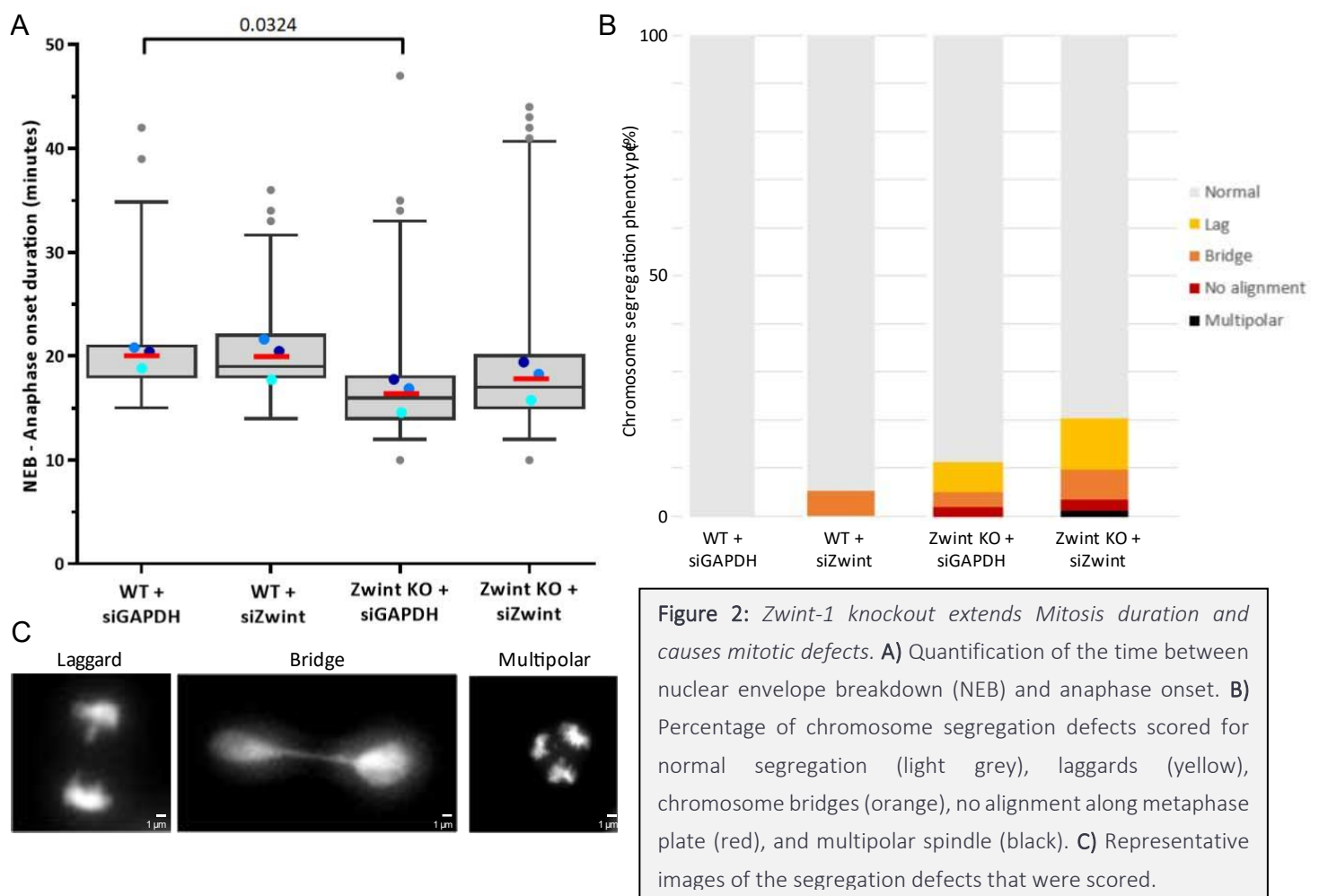


Figure 1: *Zwint-1* can be successfully mutated to prevent its localization to kinetochore. **A)** Representative images of MG132-treated (1h) cells of WT and *Zwint-1* KO. Bottom row displays staining where no primary antibody specific for *Zwint-1* was added. *Zwint-1* is shown in green, while kinetochore marker CENP-C is shown in magenta. The merge column (right) shows additional staining for Tubulin (red) and DAPI (blue). **B)** Quantification of kinetochore localization of *Zwint-1* in MG132-treated cells. Additionally, localization following RNAi depletion of GAPDH and *Zwint-1* in both WT and *Zwint-1* KO cell lines is displayed. Similar to all graphs (unless noted otherwise), colored dots represent separate experimental repeats, and the most outlying 2.5% of data points are displayed outside the deviation 'whiskers'. Localization values are normalized to WT for *Zwint-1* KO lines, and to WT + siGAPDH for RNAi lines. P values of an unpaired t test are calculated between the averages of the several experimental repeats. Red bars indicate standard deviation between averages of repeats. **C)** Representative images of noco-treated (16h) cells of WT and *Zwint-1* KO. Additionally, localization following RNAi depletion of GAPDH and *Zwint-1* in both WT and *Zwint-1* KO cell lines is displayed. **D)** Quantification of noco-treated cells of the



Furthermore, live imaging mitosis allows the ability to score chromosome segregation on possible segregation defects. Chromosome segregation was checked for four different types of defects: laggards (lag), bridges, no metaphase plate alignment, multipolar spindle (Figure 2C) [66]. A laggard describes the phenomenon that during anaphase, one or more of the chromosomes stay on the metaphase plate, while the others travel towards the spindle poles. These lagging chromosomes can either still travel towards a pole a few moments later, or be abandoned during telophase and end up as micronuclei. Bridges describe how during anaphase, one or more chromosomes or chromatids are stretched between the separating chromosome masses. These bridges often break, leading to incomplete chromosomes in the daughter cells. No alignment describes a scenario where during prometaphase, the chromosomes have trouble aligning to the metaphase plate, ultimately fail to do so, and anaphase is started anyway. In order for anaphase to be started, the SAC, which should prevent anaphase onset until proper biorientation is established, has to be overruled in some way. No proper metaphase plate alignment often causes aneuploidy. Lastly, a graver mitotic defect is the occurrence of a multipolar spindle. Here, the mitotic spindle originates from 3 or more spindle poles, as opposed to the usual 2. Therefore, during anaphase, the chromosomes can be distributed over 3 or more daughter cells, causing extreme aneuploidy which usually results in apoptosis.

Scoring the *Zwint-1* knockdown and knockout lines for these phenotypes gave interesting results, as absence of *Zwint-1* clearly results in occasional mitotic defects (Figure 2B). While the lion's share of cells is still able to divide normally, absence of *Zwint-1* gives rise to all four of the discussed defects.

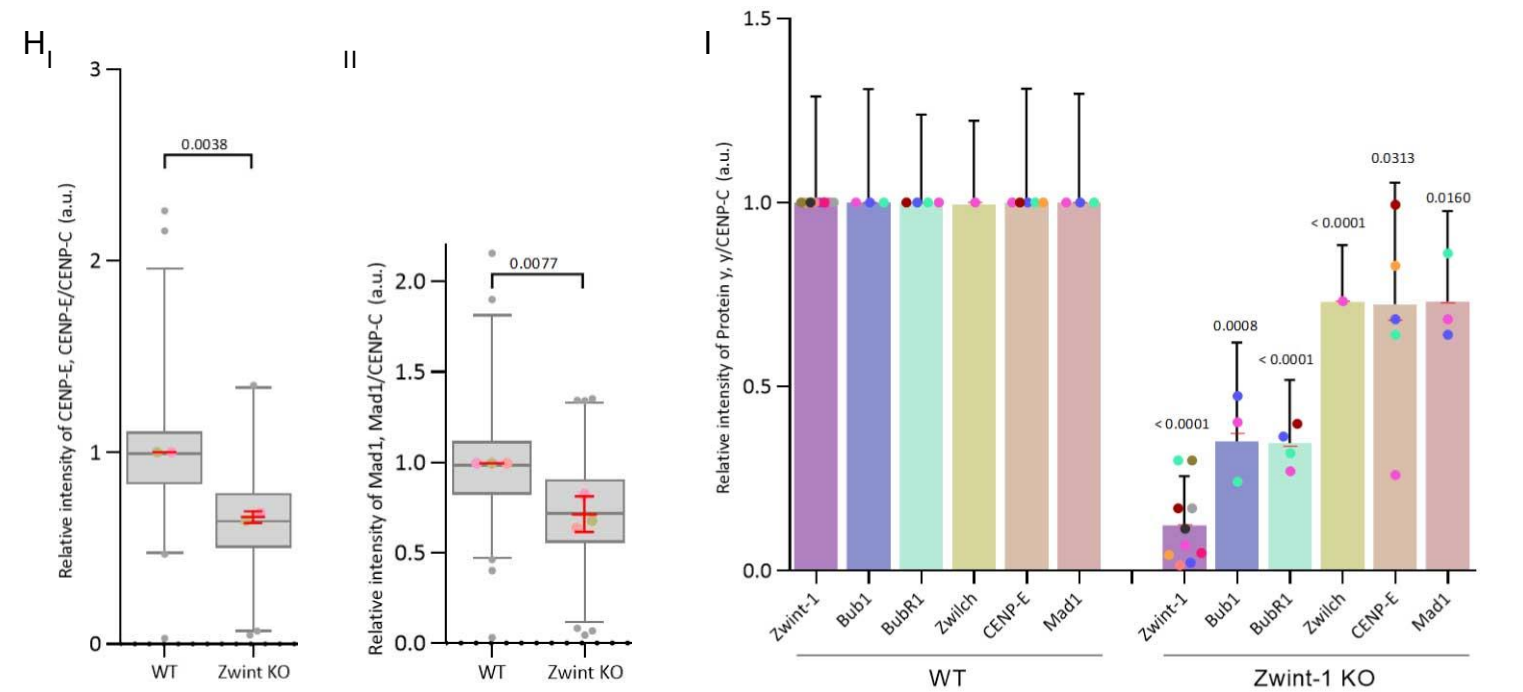
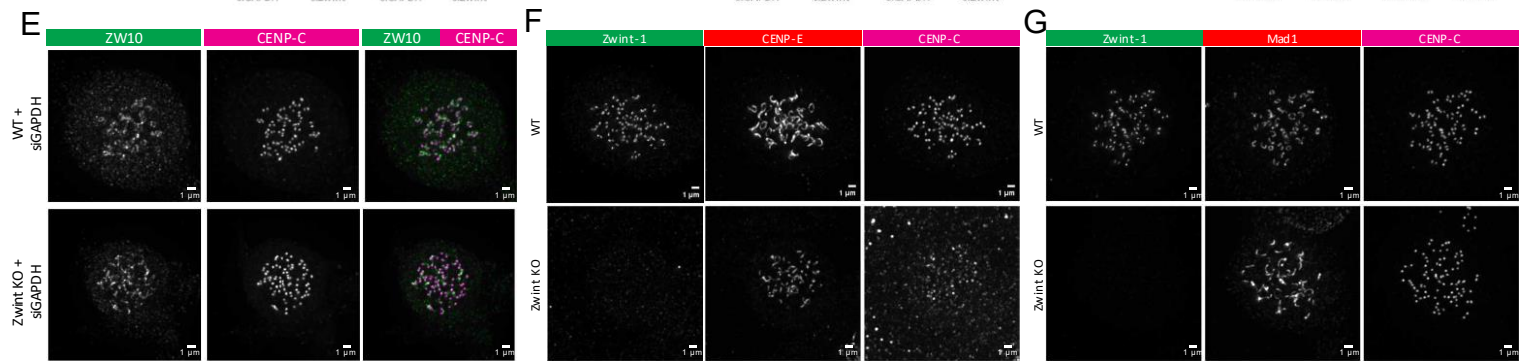
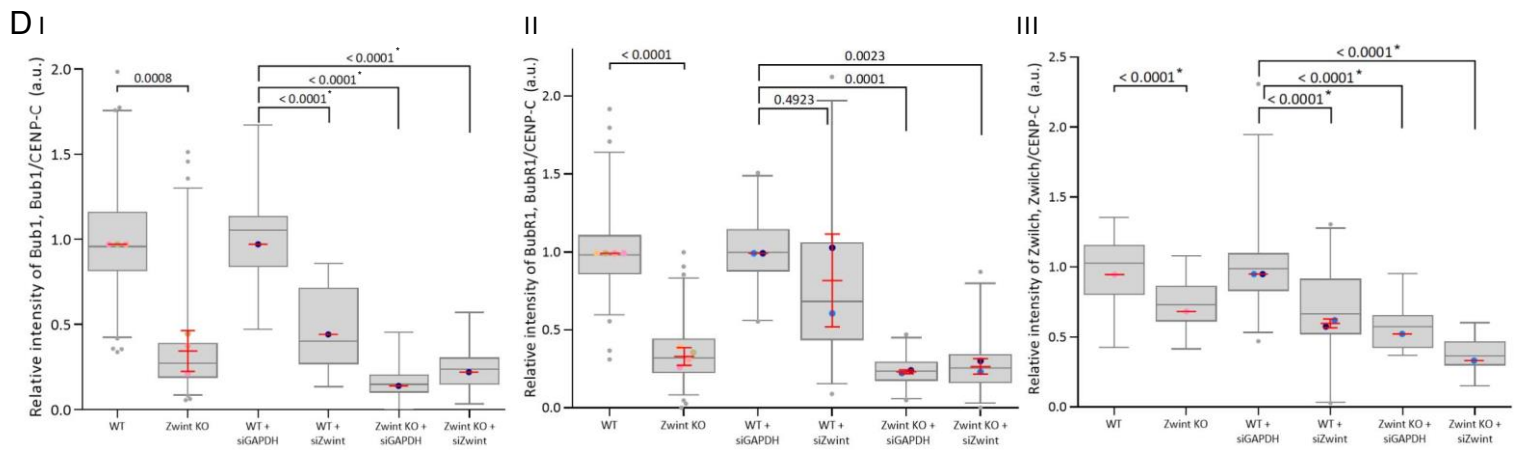
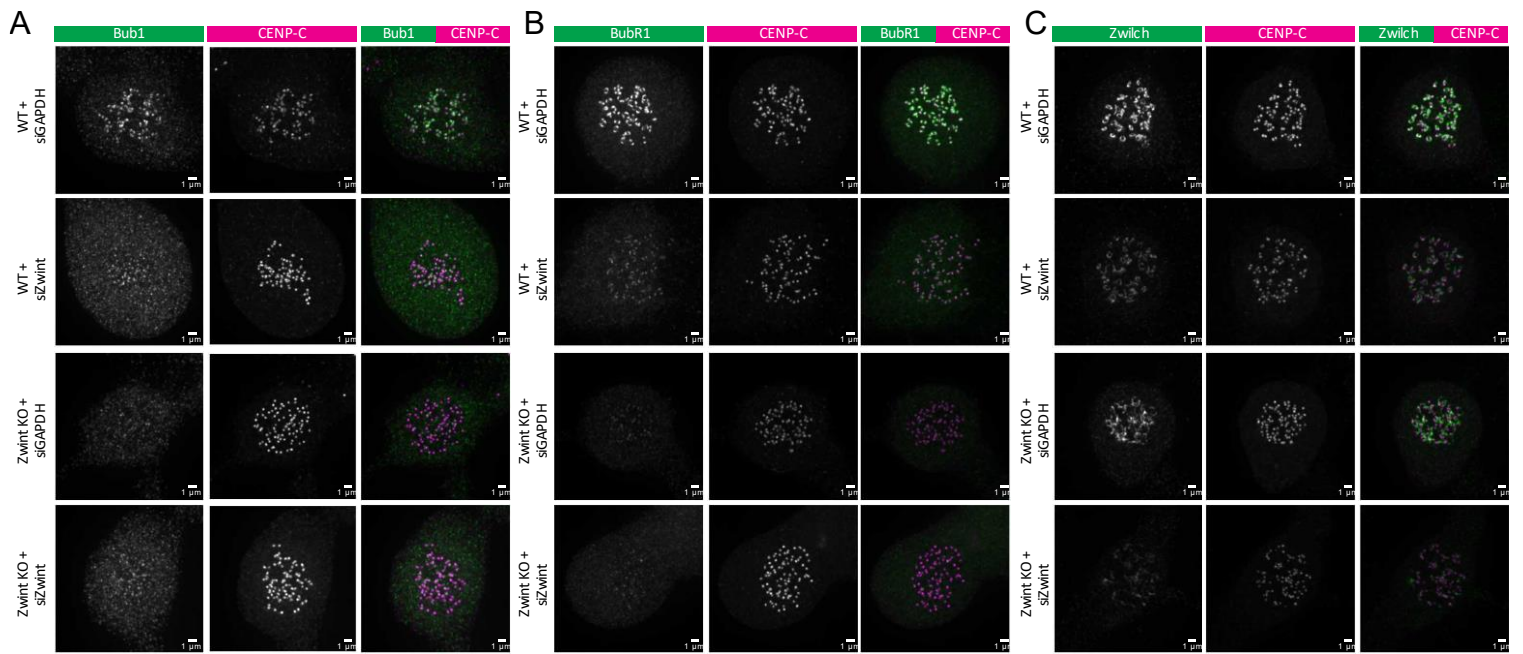


Figure 3: Localization of multiple kinetochore proteins is impaired following Zwint-1 knockout. **A,B,C)** Representative images of noco-treated cells of WT and Zwint-1 KO and additional RNAi for Zwint-1 or GAPDH. The kinetochore protein of interest (respectively Bub1, BubR1, Zwilch) is shown in green, while kinetochore marker CENP-C is shown in magenta. Both channels are overlaid in the right column. **D)** Quantification of kinetochore localization of Bub1 (i), BubR1 (ii) and Zwilch (iii) in the conditions displayed above. P values indicated with an asterisk (*) were calculated via an unpaired t test between all data points for a single or duplicate of experiments, as repeat experiments were yet to be conducted. **E)** Representative images of noco-treated cells stained for ZW10. **F, G)** Representative images of noco-treated cells stained for CENP-E (E) and Mad1 (G) (both red). Separate antibody host animals gave the opportunity to co-stain for Zwint-1 (green). **H)** Quantification of the kinetochore localization of CENP-E (i) and Mad1 (ii) in WT and Zwint-KO as displayed in F and G. **I)** Collection of the quantification data from several kinetochore proteins affected by Zwint-1 knockout. Coloured bars represent a different kinetochore protein, as indicated on the y axis. Black bars represent standard deviation of the whole dataset. Red stripes indicate the mean of the averages of the data from experiment repeats.

Localization of multiple kinetochore proteins is impaired following Zwint-1 knockout

The next step was to search for the underlying cause of the decreased mitosis duration and subsequent mitotic defects. How did Zwint-1 knockout affect the overall kinetochore to result in such alterations? To visualize this, immunofluorescence for kinetochore proteins downstream of Zwint-1 (and therefore KNL1) was conducted. Here, the experiments that were done in cells treated by nocodazole are discussed, as these mimic the kinetochores in an unattached state. Quantification data of BubR1 localization to the kinetochore in MG132-treated cells can be found in **supplementary figure 1** for comparison. As described in the introduction, Bub1 is one of the first proteins recruited to KNL1 via MELT site phosphorylation. When assessing the localization of Bub1 under Zwint-1 knockdown and knockout, a clear decrease can be seen (**Figure 3A**). Given their relation, the kinetochore localization of BubR1 follows a very similar pattern to Bub1 (**Figure 3B**). When quantified using the same kinetochore colocalization macro as before, the effect becomes even more clear. In absence of Zwint-1, Bub1 and BubR1 only localize minimally to the kinetochore, as Zwint-1 knockout decreases their localization to only ~25-30% compared to WT (**Figure 3Di, ii**).

Furthermore, RZZ complex component Zwilch also showed decreased kinetochore localization under Zwint-1 absence, albeit less profound (**Figure 3C, 3Diii**). Interestingly however, RZZ component ZW10 did not show altered kinetochore localization under Zwint-1 absence (**Figure 3E, supplementary figure 2**). While requirement of Zwint-1 for ZW10 localization was already debunked, and Bub1 was identified as the recruiter for the RZZ complex, the decreased Bub1 localization did not affect ZW10.

Given the impact of Zwint-1 depletion on the close interactors of KNL1 and therefore the kinetochore structure, it is interesting to also assess possible changes in localization of fibrous corona proteins. As described in the introduction, CENP-E and Mad1 are both important fibrous corona proteins, and both show an impaired localization to the kinetochore when Zwint-1 is knocked out (**Figure 3F,G, Hi,ii**). This decrease shows a significant effect of Zwint-1 knockout on the fibrous corona and therefore the whole structure and possibly the functioning of the outer kinetochore. The altered fibrous corona will be analysed more closely later. Taken together, many of the kinetochore proteins downstream of Zwint-1 and KNL1 exhibit significantly decreased localization to the kinetochore (**Figure 3I**). This argues for a role of Zwint-1 in stabilizing the structure and integrity of the kinetochore.

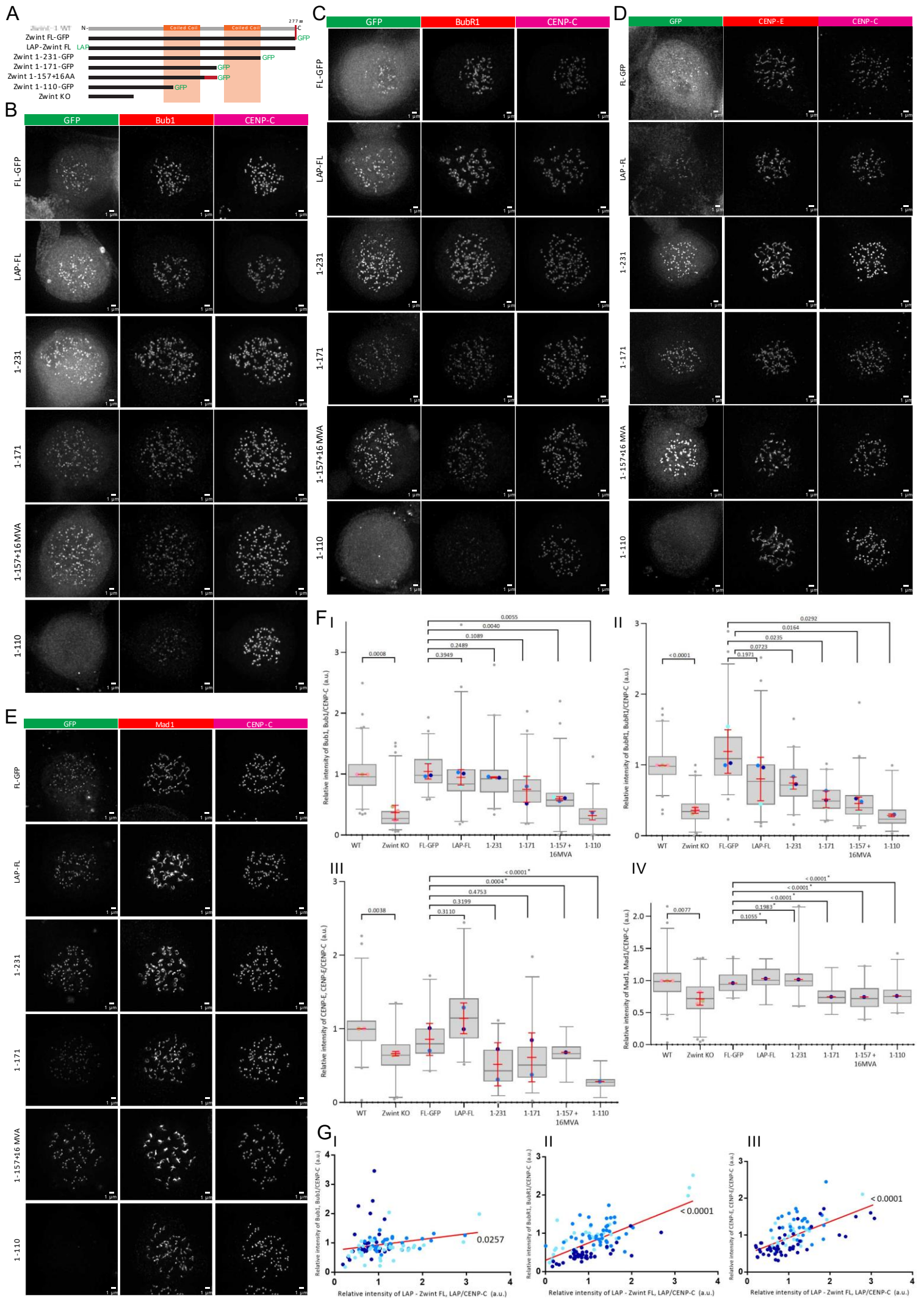


Figure 4: *Expression Zwint-1 constructs in Zwint-1 KO line recovers kinetochore protein localization.* **A)** Schematic representation of Zwint-1 WT, the knockout mutant and the expressed constructs. Coiled coil domains of Zwint-1 are indicated in orange. GFP/LAP-tags are illustrated in green. **B,C,D,E)** Representative images of noco-treated cells of from the construct expression lines. GFP expression and localization is shown in green. The kinetochore protein of interest (respectively Bub1 (**B**), BubR1 (**C**), CENP-E (**D**), Mad1 (**E**)) is shown in red, and kinetochore marker CENP-C is shown in magenta. **F)** Quantification of kinetochore localization of the protein of interest (respectively Bub1 (**i**), BubR1 (**ii**), CENP-E (**iii**), Mad1 (**iv**)) in the conditions and with the constructs displayed above. **G)** Comparison between kinetochore localization of the protein of interest (respectively Bub1 (**i**), BubR1 (**ii**), CENP-E (**iii**), and localization of the LAP-Zwint full length construct. Dots represent kinetochore localization values of both parameters, and the colours represent repeated experiments. Regression line was calculated regarding the total population of datapoints for each protein.

Expression Zwint-1 constructs in Zwint-1 KO line recovers kinetochore protein localization

To confirm that the observed destabilization of the kinetochore was due to the knockout of Zwint-1, Zwint-1 rescue lines were set up. The aim was to re-establish WT levels of kinetochore protein localization by expressing Zwint-1 constructs of varying lengths in the Zwint-1 KO line (**Figure 4A**). Two full-length (FL) constructs were used, one containing a GFP tag C-terminally, while the other contained a LAP tag N-terminally, in order to control for possible interference of the tag with localization or function of the Zwint-1 construct. The partial Zwint-1 constructs had stepwise decreases in amino acid chain length.

A stable expression of the constructs was observed in the Zwint-1 KO RPE1 line (**Figure 4B,C,D,E**, left columns). Interestingly, the 1-110 construct did not localize to kinetochores, while the larger constructs did. Looking at the behaviour of Bub1 in these rescue lines, a distinct kinetochore localization is seen under the various constructs (**Figure 4B**). The quantified data shows how the full-length and larger constructs have the ability to rescue Bub1 localization to WT levels, while Bub1 localization under the non-localizing construct is similar to that under Zwint-1 KO (**Figure 4Fi**). The quantified data further reveals that the 1-231 construct is able to restore Bub1 localization similar to the FL constructs, while the 1-171 and MVA constructs achieve less restoration of Bub1 localization in a stepwise fashion. It is expected that BubR1 again follows the same pattern of restoration in the rescue lines. This indeed was the case, as shown by both the immunofluorescence and quantified data (**Figure 4C, Fii**).

To see whether the altered fibrous corona protein localization could also be rescued using the rescue constructs, CENP-E and Mad1 were also analysed. In the immunofluorescence images, both CENP-E and Mad1 are seen localizing to the kinetochores, however it is difficult to gauge the difference between the different constructs (**Figure 4D,E**). However, when quantified, these differences become clearer. For CENP-E, we see a rescue of kinetochore localization due to the FL constructs. However, for the partial constructs differences are difficult to assess as the data from separate experiments is far apart (**Figure 4Fiii**). As for Mad1, the FL constructs, as well as the 1-231 construct, rescue localization to WT levels, whilst the rest of the constructs don't (**Figure 4E, Fiv**). Note that the Mad1 construct relocalization data, and some of the CENP-E data as well, are based on a single experiment, and therefore need to be repeated to confirm the observation.

A further confirmation that the Zwint-1 constructs can rescue the localization of the kinetochore proteins can be found when analysing the GFP localization data. Some variation was found in the level of GFP at the kinetochore, probably due to varying levels of construct expression between cells of the population (**Figure 4B,C,D,E**, left columns). The level of localization of the kinetochore protein can be

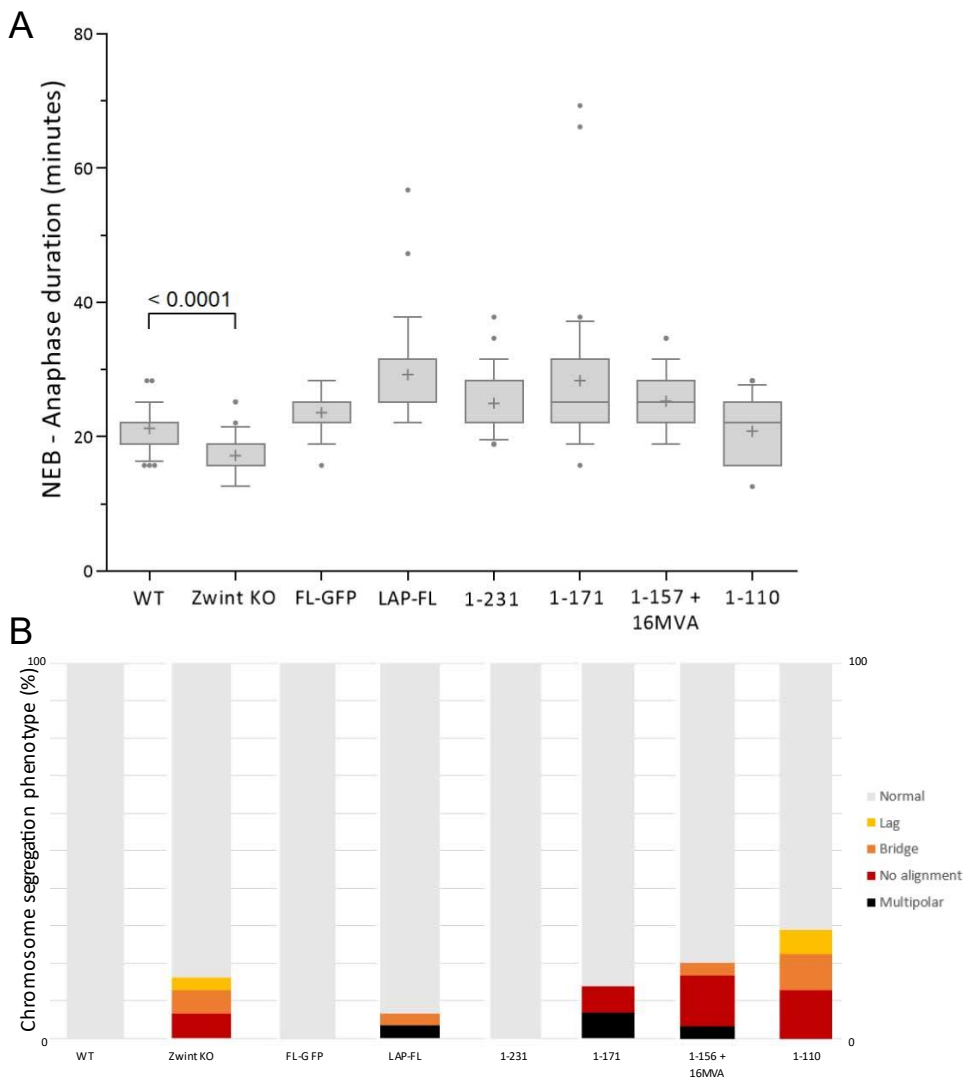


Figure 5: *Zwint-1* re-expression rescues mitotic defects.

A) Quantification of the time between nuclear envelope breakdown (NEB) and anaphase onset in WT, *Zwint-1* KO, and rescue construct cell lines.

B) Percentage of chromosome segregation defects scored for normal segregation (light grey), laggards (yellow), chromosome bridges (orange), no alignment along metaphase plate (red), and multipolar spindle (black).

analysed with regard to this varying level of GFP localization. By doing this for the LAP – *Zwint-1* FL construct, it is observed that higher localization of the construct also brings with it a higher localization of the kinetochore protein in that cell (**Figure 4G**, other constructs are found in **supplementary figure 3**). This further shows how re-expressing of *Zwint-1* constructs can rescue the kinetochore stability that was disturbed by *Zwint-1* KO.

Zwint-1 re-expression rescues mitotic defects

The next question is whether rescuing kinetochore localization of the outer kinetochore proteins, also rescues the previously described effects of *Zwint-1* KO on mitosis. Again, NE breakdown until anaphase onset was analysed. While a clear difference between WT and *Zwint-1* KO can be seen again, the rescue lines all exhibit a longer duration when compared to WT (**Figure 5A**). Note that this data is based on a single experiment, and therefore needs to be repeated before drawing concrete conclusions. When scoring the mitotic defects in the rescue lines however, interesting differences arise (**Figure 5B**). Similar to previous observations, the *Zwint-1* KO line shows multiple segregation defects. The FL and 1-231 constructs appear able to prevent these defects, while the 1-171 and MVA constructs show occurrence of defects. The non-localizing 1-110 construct exhibits the most chromosome segregation defects. While these findings still require adequate repetition, the initial results indicate that expression of the *Zwint-1* constructs in the *Zwint-1* KO line can rescue the segregation defects.

Interkinetochore distance and fibrous corona formation are affected following Zwint-1 knockout

Lastly, a closer look is taken at the behaviour of the fibrous corona under Zwint-1 KO conditions. As described in the introduction, the fibrous corona is a crescent-shaped body of proteins around unattached kinetochores, for which Mad1 can be used as marker (**Figure 6A**). While the Zwint-1 KO line still shows formation of the fibrous corona around the kinetochores, the shape and intensity is different. Zooming in on the Mad1 signal, the WT condition shows ring-like structures between the kinetochore, displaying the impressive structure that the fibrous corona forms (**Figure 6Ci**). In the Zwint-1 KO condition this structure changes significantly, as full rings rarely form and crescent shapes seem elongated and disturbed (**Figure 6Cii**). Furthermore, the fibrous coronae seem to fuse together and overlap in signal in the Zwint-1 KO condition, which is not observed in WT cells. Lastly, an interesting observation that becomes clear in the zoomed-in images, is the difference in distance between the kinetochores of sister chromatids (**Figure 6B**). While WT sister chromatid kinetochores are close together and form ring-like fibrous corona structures, these paired kinetochores are further apart in the Zwint-1 KO condition. This phenomenon was quantified using ImageJ line measurements, showing how the Zwint-1 KO condition significantly increases interkinetochore distance by ~10% (**Figure 6D**).

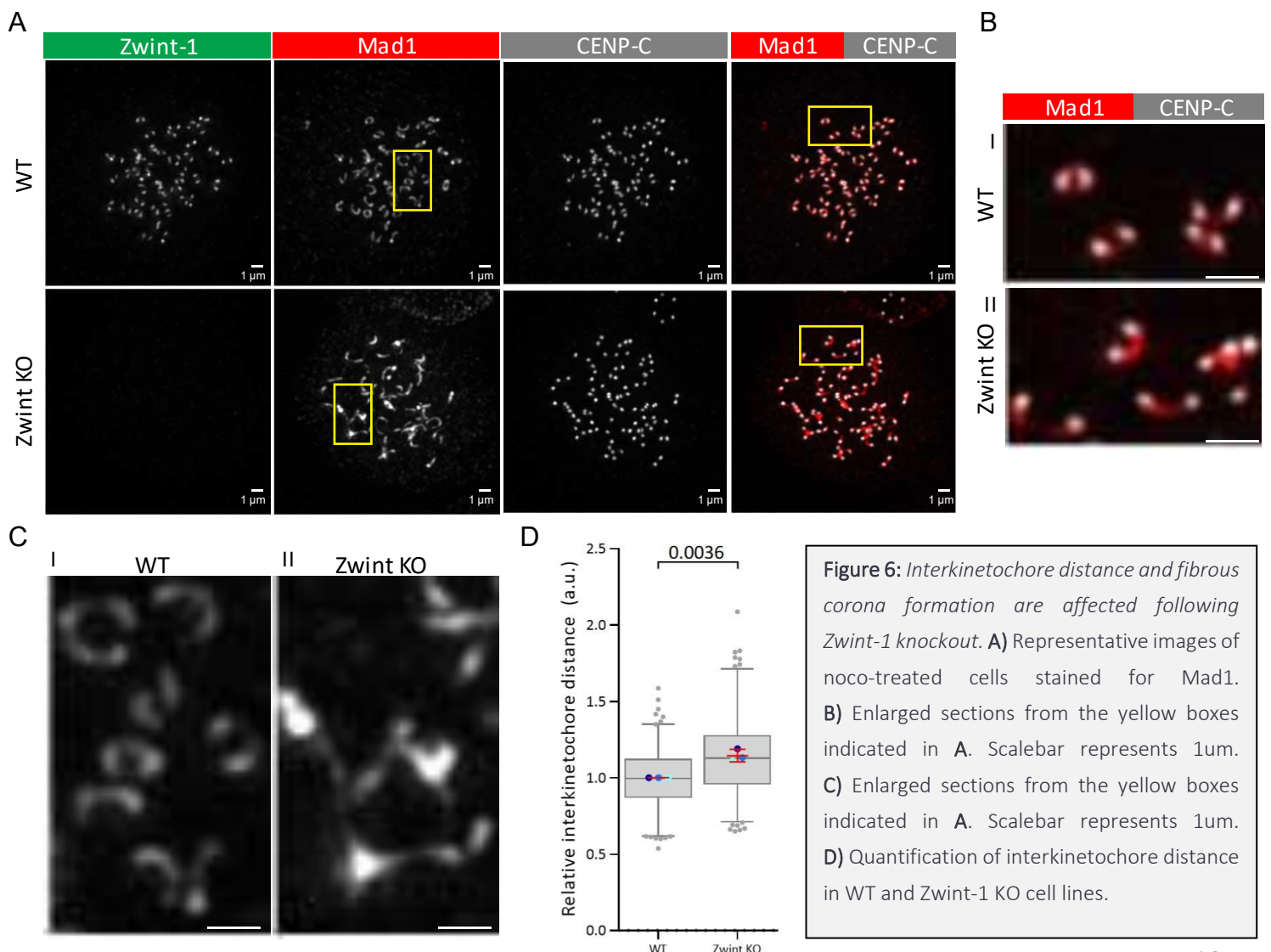


Figure 6: *Interkinetochore distance and fibrous corona formation are affected following Zwint-1 knockout.* **A)** Representative images of noco-treated cells stained for Mad1. **B)** Enlarged sections from the yellow boxes indicated in **A**. Scalebar represents 1 μ m. **C)** Enlarged sections from the yellow boxes indicated in **A**. Scalebar represents 1 μ m. **D)** Quantification of interkinetochore distance in WT and Zwint-1 KO cell lines.

Conclusions & discussion

Zwint-1 was initially identified as the recruiter of ZW10 to the kinetochore [53,54]. However, it was since shown how ZW10 mutants that fail to bind to Zwint-1 could still (less stably) localize to kinetochores [55]. More recently, it was shown how RZZ recruitment to the kinetochore depends on Bub1 instead of Zwint-1 [56]. The stable nature of Zwint-1 in the kinetochore, combined with its direct interaction with ZW10 and KNL1, point to a possible structural role for Zwint-1 in kinetochore assembly [57,58].

In this work, the uncertainties regarding the role and significance of Zwint-1 in the kinetochore are addressed. An RPE-1 line containing a Zwint-1 knockout is presented, which expresses a Zwint-1 1-59aa mutant at under 6% of the WT Zwint-1 mRNA level. This mutant doesn't localize to the kinetochore and therefore the kinetochores in the knockout line will assemble without having access to functioning and localizing Zwint-1 (**Figure 1**). While the effect of RNAi knockdown of Zwint-1 in human cells has been explored before, a human cell line with a Zwint-1 knockout provides an interesting platform to study the role of Zwint-1 in the kinetochore.

Interestingly, the Zwint-1 knockout line mitosis showed a time decrease between nuclear envelope breakdown and anaphase onset (**Figure 2A**). Additionally, several different chromosome segregation defects were observed in cells under Zwint-1 knockout (**Figure 2B**). These findings indicate significant consequences of Zwint-1 knockout for the cell and its genomic integrity, and are consistent with a previous study in HeLa cells which described a defective spindle checkpoint after RNAi Zwint-1 depletion [57]. The chromosome segregation defects were successfully restored by expressing full length Zwint-1 constructs in the knockout line (**Figure 5B**).

Immunofluorescence assays on the localization of the outer kinetochore proteins revealed how many of the outer kinetochore proteins downstream of Zwint-1 and KNL1 show decreased localization to the kinetochore upon Zwint-1 knockout. Strongly impaired kinetochore localization of Bub1 and BubR1 was observed (**Figure 3A,B,Di-ii**). These observations were successfully rescued and restored to WT levels by expressing full length Zwint-1 constructs in the knockout line (**Figure 4A,B,C,Fi-ii**). Interestingly, while Zwilch localization was also affected by Zwint-1 KO, fellow RZZ complex subunit ZW10 remained unaffected (**Figure 3C,Diii,E**). Direct interactions between Zwint-1 and the Bubs were never found, and as Zwint-1 is such a relatively small protein, it would be unlikely to directly interact with these proteins. Instead, Zwint-1 is more likely to be involved in assisting kinetochore assembly, most prominently via its interaction with scaffolding protein KNL1. KNL1 is recruited to the kinetochore via binding to both Mis12 and Zwint-1, and both interactions are mediated by RWD repeats [61]. Zwint-1 RNAi depletion in HeLa cells leads to ~60% reduction of KNL1 localization to the kinetochore, while KNL1 depletion stops kinetochore localization of both Zwint-1 and Mis12, showing a codependency between these proteins for localization to the kinetochore [56,62]. Given that Zwint-1 depletion leads to decreased KNL1 localization, it can be expected that in the Zwint-1 KO RPE1 cell line, KNL1 localization is also

decreased, possibly more severely. Unfortunately, specific staining for KNL1 in RPE1 cells was not achieved here, and efforts to produce fluorescently tagged KNL1 constructs are still ongoing. Information on the behaviour of KNL1 under Zwint-1 KO could further confirm the hypothesis that Zwint-1 has a stabilizing role for KNL1. If Zwint-1 KO indeed depletes KNL1 localization to the kinetochore, the phenotype could be similar to that observed under RNAi depletion of KNL1. This would also explain many of the consequences observed in the Zwint-1 KO line, as KNL1 depletion in HeLa cells showed to decrease Bub1, ZW10, Rod and Mad1 localization to the kinetochore [56,62].

Furthermore, the Zwint-1 knockout seems to affect fibrous corona formation. While localization of RZZ components show variability as discussed above, other fibrous corona proteins CENP-E and Mad1 indeed exhibit affected kinetochore localization under Zwint-1 knockout (**Figure 3F,G,H**). Decreased localization was successfully rescued and restored to WT levels by expressing full length Zwint-1 constructs in the knockout line (**Figure 4A,D,E,Fiii-iv**). This is consistent with a previous study showing how in HeLa siZwint decreased Mad1 localization by ~40% [62]. Additionally, a different study showed a ~20% decrease in Mad2 localization in HeLa cells under Zwint-1 depletion [58].

Not only is the signal on the kinetochore decreased, the crescent structure of the fibrous corona is also affected (**Figure 6A,C**). The cells seem less able to form proper fibrous corona structures, and the structures that do form seem to fuse together. Fusion of fibrous coronae is a phenomenon that hasn't been investigated in detail yet, and more research into interactions between fibrous corona structures might explain why unattached kinetochores disturbed by Zwint-1 knockout are more likely to fuse together. Another interesting observation is the significant increase between kinetochores of sister chromatids under Zwint-1 knockout (**Figure 6B,D**). As all kinetochores are in an unattached state, and nocodazole treated, they should not be under tension from microtubules. This argues for structural changes, possibly amongst the CENPs, which have not yet been described as a result from KNL1 or Zwint-1 alterations.

Expression of Zwint-1 constructs in the knockout line gave the opportunity to assess whether specific parts of the Zwint-1 protein are needed for restoration of the kinetochore stability. The constructs were designed to include or exclude the coiled coil structures important for Zwint-1 interactions with KNL1 and ZW10 (**Figure 4A**). Initial results show how the Zwint-1 1-231, which includes both coiled coil structures, is able to restore localization of kinetochore proteins to similar levels as full length constructs (**Figure 4B,C,D,E,F**). The smaller constructs are not able to restore localization to this extent. The 1-110 construct, which contains no complete coiled coil domain, loses the ability to localize to the kinetochore. Higher expression and/or kinetochore localization of a full-length construct also provokes higher localization of kinetochore proteins, which is consistent with the hypothesis that these Zwint-1 constructs will stabilize the kinetochore (**Figure 4G, supplementary figure 3**). Although more experiment repeats and analysis of additional kinetochore proteins are needed for confirmation, these initial observations strengthen the role of the coiled coil domains in Zwint-1 for its interaction with the kinetochore.

Taken together, these findings illustrate the undeniable relevance of Zwint-1 in the kinetochore. The coiled coil domains of Zwint-1 are important for its kinetochore localization and subsequent interaction with other kinetochore proteins. Zwint-1 absence disturbs the kinetochore in a similar fashion as KNL1 depletion, arguing for a possible role for Zwint-1 in stabilizing KNL1 in its scaffolding role and the many interactions with kinetochore proteins.

Over the past few years, several studies have come out describing the possible role of Zwint-1 in cancer. Zwint-1 was reported to be overexpressed in numerous types of cancer, and this could be related to the prognosis of the tumour [67,68,69,70,71,72]. Therefore, Zwint-1 was identified as a possible prognostic biomarker and potentially even a therapeutic target [73,74,75]. Whereas it is difficult to translate these studies to the findings of this report, the significance for Zwint-1 in the kinetochore is again displayed. Further research and new insights in the mechanics of Zwint-1 and its interaction with KNL1 to stabilize the kinetochore structure will shed light on the details of kinetochore assembly, providing essential information to fully understand the consequences of Zwint-1 deregulation or mutations.

Materials and Methods

Cell culture and transfection

The RPE1 Flp-In T-Rex cell lines were cultured in DMEM/F12 (1:1)(1x) + GlutaMAX™ cell culture medium (Thermo Fisher) with 10% tetracycline-free fetal bovine serum (FBS)(Bodingo), supplemented with 1% penicillin-streptomycin (PS)(Sigma-Aldrich; 50 µg/ml) and hygromycin (200 µg/ml) or puromycin (1 µg/ml) depending on possible selection cultures. Cells were incubated at 37°C with 5% CO₂. Cell lines were split to 5% confluency every 5 days, and frequently tested for contaminations. Plasmids were transfected using and FuGENE HD transfection reagent (Promega) according to the manufacturer's instructions. RPE1 FlpIn T-Rex cell lines were transfected with PX459 constructs, which were later expressed by addition of 1 µg/ml doxycycline for 24 h. To prepare the cell lines for live imaging, cells were plated to 24-well plates and H2B-scarlet was transfected using a lentiviral vector. To knock down Zwint-1, cells were transfected with 40 nM siRNA diluted in OPTIMEM (Thermo Fisher) against Zwint-1 (custom mix against all 8 exons of ZWINT gene) or siGAPDH (Thermo Fisher Scientific; D-001830-01-50) using HiPerfect (Qiagen) according to manufacturer's instructions.

Live-cell imaging

For live-cell imaging experiments, cells were plated in 24-well plates with black sidings and glass underside (Greiner Bio-One). Imaging was done via DIC microscopy on a Nikon Ti-E motorized microscope equipped with a Zyla 4.2 Mpx sCMOS camera (Andor) and a 40x 1.30 NA objective lens (Nikon). Fluorescence excitation came from a Spectra X LED illumination system (Lumencor), with Chroma-ET filter sets. Cells were kept at 37°C and 5% CO₂ using a cage incubator and Boldline temperature/CO₂ controller (OKO-Lab). Images were acquired every 1 to 2 minutes without binning and

processed by Nikon Imaging Software (NIS). Analysis of live-cell imaging experiments was carried out with ImageJ software and time in mitosis was defined as the time between nuclear envelope breakdown and anaphase onset. Mitosis time data was compiled and processed using Microsoft Office Excel, and graphs were created using GraphPad Prism 6. Chromosome segregation defects were scored manually and column diagrams were created using Microsoft Office Excel.

Immunofluorescence

For fixed-cell immunofluorescence microscopy, cells were plated on round 12-mm coverslips and subsequently fixated using 100% methanol in -20°C for 5 minutes, or 4% paraformaldehyde for 10 minutes. Coverslips were then washed three times with cold PBS, permeabilized with 0.1% Triton X-100 in PBS for 2 minutes, and then blocked with 2% BSA in PBS for 20 minutes at room temperature. Blocked coverslips were then incubated with primary antibodies diluted in 2% BSA in PBS-0.05% Tween (30ul per slide) for 16 h at 4°C , washed five times with PBS containing 0.05% Tween, and incubated with secondary antibodies diluted in PBS-0.05% Tween (20ul per slide) for 1 hour at room temperature. Coverslips were then washed five times with PBS containing 0.05% Tween, incubated with DAPI 1:1000 for 2 minutes, and washed again twice with PBS containing 0.05% Tween. Next, the coverslips were dipped in both 70% and 100% ethanol respectively, before air drying in darkness. Lastly, the coverslips were mounted using Prolong Gold antifade (Invitrogen). All fixed immunofluorescence images were acquired on a deconvolution system (DeltaVision Elite; Applied Precision/GE Healthcare) with a 100x/1.40 NA UPlanSApo objective (Olympus) and a 1Mpx CoolSnapHQ2 CCD camera (Photometrics) using SoftWorx 6.0 software (Applied Precision/GE Healthcare). All images of a specific protein were acquired with illumination settings specific for that protein and identical across experiments. All images of GFP constructs in simultaneously stained experiments were acquired with identical illumination settings. Deconvolution is applied to all images and maximum projection is shown in figures.

Image quantification and data analysis

For analysis and quantification of immunostaining, the ImageJ2 software was used. For analysis of the Zwint-1 construct-expressing cell lines, only cells expressing visible and comparable levels of exogenous protein were selected for analysis. Kinetochores localization was quantified using an automated macro. In brief: the DAPI channel is selected after a “default dark” auto threshold is run. This selection is enlarged by 5 pixels to form the area in which kinetochores are quantified. The CENP-C channel is deconvolved and selected after a “default dark” auto threshold is run. This area is enlarged by 1 pixel to form the area regarded as ‘localized to the kinetochore’. Unmodified signal from the channel from the protein of interest is measured on pixels with unmodified signal from the CENP-C channel within both areas to quantify kinetochore localization of the protein of interest. Interkinetochore distance was measured using the “line measurement” tool in ImageJ. Quantification data was compiled and processed using Microsoft Office Excel, and graphs were created using GraphPad Prism 6. For all graphs except the column graphs, Prism’s ‘box and whiskers’ display was used, with the most outlying 2.5% of data points displayed outside the deviation ‘whiskers’. Statistical significance was analysed by

calculating the P value of an unpaired t test within Prism 6 between the averages of several experimental repeats. P values indicated with an asterisk (*) were calculated via an unpaired t test between all data points for the single experiment, as repeat experiments were yet to be conducted.

Antibodies for immunostaining

The primary and secondary antibodies used for immunostaining are displayed in *table 1* and *table 2*.

Table 1: Primary antibodies used for immunostaining

Antibody	Host	Clonality	Company	Order nr.
Zwint-1	Rabbit	Polyclonal	Abcam	ab71982
Tubulin	Mouse	Monoclonal	Sigma-Aldrich	t5168
CENP-C	Guinea pig	Polyclonal	MBL International	PD030
GFP	Mouse	Monoclonal	Roche	12-814-460-001
Bub1	Rabbit	Polyclonal	Bethyl	A300-373 A-1
BubR1	Rabbit	Polyclonal	Bethyl	A300-386 A
ZW10	Rabbit	Polyclonal	Abcam	ab21582
MAD1	Rabbit	Polyclonal	Santa Cruz	sc-67337
CENP-E	Mouse	Polyclonal	Abcam	ab50987

Table 2: Secondary antibodies used for immunostaining

Antibody	Signal	Host	Clonality	Company	Order nr.
anti-Rabbit	Alexa Fluor 488	Goat	Polyclonal	Invitrogen	A-11034
anti-Mouse	Alexa Fluor 488	Goat	Polyclonal	Invitrogen	A-11029
anti-Mouse	Alexa Fluor 568	Goat	Polyclonal	Invitrogen	A-11031
anti-Guinea pig	Alexa Fluor 647	Goat	Polyclonal	Invitrogen	A-21450
GFP booster	Atto 488	-	-	Chromotek	gba488

Acknowledgements

Most importantly, I want to thank Jingchao Wu for his guidance, help and supervision throughout this project. I am extremely grateful for all his dedication and support in the experiments, data analysis and reviewing of the manuscript. Furthermore, I would like to thank Geert Kops for offering me an unforgettable opportunity to get inundated with research in his research group and develop myself in his lab. Despite the rollercoaster of the past year on a global and personal level, my experience in the group was better than I could've dreamt of, owing to the inspiring hospitality, support and social nature of all members in the Kops group, for which I want to thank each and every member sincerely.

References

- ¹ Santaguida, S., & Amon, A. (2015). Short-and long-term effects of chromosome mis-segregation and aneuploidy. *Nature reviews Molecular cell biology*, *16*(8), 473-485.
- ² Pesenti, M. E., Weir, J. R., & Musacchio, A. (2016). Progress in the structural and functional characterization of kinetochores. *Current opinion in structural biology*, *37*, 152-163.
- ³ Santaguida, S., & Musacchio, A. (2009). The life and miracles of kinetochores. *The EMBO journal*, *28*(17), 2511-2531.
- ⁴ Fukagawa, T., & Earnshaw, W. C. (2014). The centromere: chromatin foundation for the kinetochore machinery. *Developmental cell*, *30*(5), 496-508.
- ⁵ Musacchio, A., & Desai, A. (2017). A molecular view of kinetochore assembly and function. *Biology*, *6*(1), 5.
- ⁶ McKinley, K. L., & Cheeseman, I. M. (2016). The molecular basis for centromere identity and function. *Nature reviews Molecular cell biology*, *17*(1), 16-29.
- ⁷ Hara, M., & Fukagawa, T. (2017). Critical foundation of the kinetochore: the constitutive centromere-associated network (CCAN). In *Centromeres and Kinetochores* (pp. 29-57). Springer, Cham.
- ⁸ Saurin, A. T. (2018). Kinase and phosphatase cross-talk at the kinetochore. *Frontiers in cell and developmental biology*, *6*, 62.
- ⁹ Hara, M., & Fukagawa, T. (2018). Kinetochore assembly and disassembly during mitotic entry and exit. *Current opinion in cell biology*, *52*, 73-81.
- ¹⁰ Cheeseman, I. M., Chappie, J. S., Wilson-Kubalek, E. M., & Desai, A. (2006). The conserved KMN network constitutes the core microtubule-binding site of the kinetochore. *Cell*, *127*(5), 983-997.
- ¹¹ Petrovic, A., Pasqualato, S., Dube, P., Krenn, V., Santaguida, S., Cittaro, D., ... & Maiolica, A. (2010). The MIS12 complex is a protein interaction hub for outer kinetochore assembly. *Journal of Cell Biology*, *190*(5), 835-852.
- ¹² Petrovic, A., Keller, J., Liu, Y., Overlack, K., John, J., Dimitrova, Y. N., ... & Rombaut, P. (2016). Structure of the MIS12 complex and molecular basis of its interaction with CENP-C at human kinetochores. *Cell*, *167*(4), 1028-1040.
- ¹³ Obuse, C., Iwasaki, O., Kiyomitsu, T., Goshima, G., Toyoda, Y., & Yanagida, M. (2004). A conserved Mis12 centromere complex is linked to heterochromatic HP1 and outer kinetochore protein Zwint-1. *Nature cell biology*, *6*(11), 1135-1141.
- ¹⁴ Ustinov, N. B., Korshunova, A. V., & Gudimchuk, N. B. (2020). Protein Complex NDC80: Properties, Functions, and Possible Role in Pathophysiology of Cell Division. *Biochemistry (Moscow)*, *85*, 448-462.
- ¹⁵ Wei, R. R., Sorger, P. K., & Harrison, S. C. (2005). Molecular organization of the Ndc80 complex, an essential kinetochore component. *Proceedings of the National Academy of Sciences*, *102*(15), 5363-5367.
- ¹⁶ Ghongane, P., Kapanidou, M., Asghar, A., Elowe, S., & Bolanos-Garcia, V. M. (2014). The dynamic protein Knl1—a kinetochore rendezvous. *Journal of cell science*, *127*(16), 3415-3423.

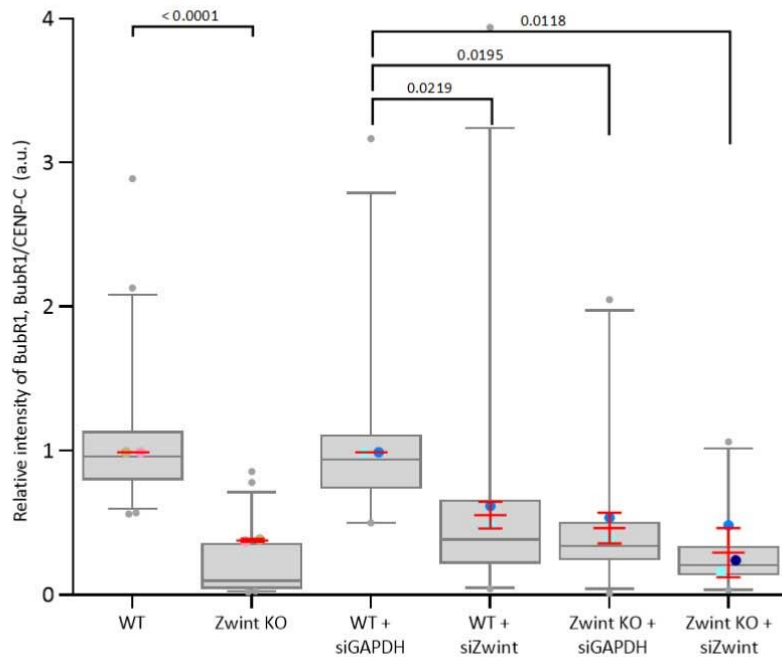
-
- ¹⁷ Sacristan, C., & Kops, G. J. (2015). Joined at the hip: kinetochores, microtubules, and spindle assembly checkpoint signaling. *Trends in cell biology*, 25(1), 21-28.
- ¹⁸ Musacchio, A. (2015). The molecular biology of spindle assembly checkpoint signaling dynamics. *Current biology*, 25(20), R1002-R1018.
- ¹⁹ Vleugel, M., Hoogendoorn, E., Snel, B., & Kops, G. J. (2012). Evolution and function of the mitotic checkpoint. *Developmental cell*, 23(2), 239-250.
- ²⁰ Kapanidou, M., Curtis, N. L., & Bolanos-Garcia, V. M. (2017). Cdc20: at the crossroads between chromosome segregation and mitotic exit. *Trends in biochemical sciences*, 42(3), 193-205.
- ²¹ Dou, Z., Prifti, D. K., Gui, P., Liu, X., Elowe, S., & Yao, X. (2019). Recent progress on the localization of the spindle assembly checkpoint machinery to kinetochores. *Cells*, 8(3), 278.
- ²² Caldas, G. V., & DeLuca, J. G. (2014). KNL1: bringing order to the kinetochore. *Chromosoma*, 123(3), 169-181.
- ²³ Schmitzberger, F., & Harrison, S. C. (2012). RWD domain: a recurring module in kinetochore architecture shown by a Ctf19–Mcm21 complex structure. *EMBO reports*, 13(3), 216-222.
- ²⁴ Pachis, S. T., & Kops, G. J. (2018). Leader of the SAC: molecular mechanisms of Mps1/TTK regulation in mitosis. *Open biology*, 8(8), 180109.
- ²⁵ Pachis, S. T., Hiruma, Y., Tromer, E. C., Perrakis, A., & Kops, G. J. (2019). Interactions between N-terminal modules in MPS1 enable spindle checkpoint silencing. *Cell reports*, 26(8), 2101-2112.
- ²⁶ Vleugel, M., Hoek, T. A., Tromer, E., Sliedrecht, T., Groenewold, V., Omerzu, M., & Kops, G. J. (2015). Dissecting the roles of human BUB1 in the spindle assembly checkpoint. *Journal of cell science*, 128(16), 2975-2982.
- ²⁷ Kiyomitsu, T., Murakami, H., & Yanagida, M. (2011). Protein interaction domain mapping of human kinetochore protein Blinkin reveals a consensus motif for binding of spindle assembly checkpoint proteins Bub1 and BubR1. *Molecular and cellular biology*, 31(5), 998-1011.
- ²⁸ Silió, V., McAinsh, A. D., & Millar, J. B. (2015). KNL1-Bubs and RZZ provide two separable pathways for checkpoint activation at human kinetochores. *Developmental cell*, 35(5), 600-613.
- ²⁹ Primorac, I., Weir, J. R., Chiroli, E., Gross, F., Hoffmann, I., Van Gerwen, S., ... & Musacchio, A. (2013). Bub3 reads phosphorylated MELT repeats to promote spindle assembly checkpoint signaling. *Elife*, 2, e01030.
- ³⁰ Vleugel, M., Omerzu, M., Groenewold, V., Hadders, M. A., Lens, S. M., & Kops, G. J. (2015). Sequential multisite phospho-regulation of KNL1-BUB3 interfaces at mitotic kinetochores. *Molecular cell*, 57(5), 824-835.
- ³¹ Yamagishi, Y., Yang, C. H., Tanno, Y., & Watanabe, Y. (2012). MPS1/Mph1 phosphorylates the kinetochore protein KNL1/Spc7 to recruit SAC components. *Nature cell biology*, 14(7), 746-752.
- ³² Shepperd, L. A., Meadows, J. C., Sochaj, A. M., Lancaster, T. C., Zou, J., Buttrick, G. J., ... & Millar, J. B. (2012). Phosphodependent recruitment of Bub1 and Bub3 to Spc7/KNL1 by Mph1 kinase maintains the spindle checkpoint. *Current Biology*, 22(10), 891-899.
- ³³ Zhang, G., Kruse, T., López-Méndez, B., Sylvestersen, K. B., Garvanska, D. H., Schopper, S., ... & Nilsson, J. (2017). Bub1 positions Mad1 close to KNL1 MELT repeats to promote checkpoint signalling. *Nature communications*, 8(1), 1-12.

-
- ³⁴ London, N., & Biggins, S. (2014). Mad1 kinetochore recruitment by Mps1-mediated phosphorylation of Bub1 signals the spindle checkpoint. *Genes & development*, 28(2), 140-152.
- ³⁵ Moyle, M. W., Kim, T., Hattersley, N., Espeut, J., Cheerambathur, D. K., Oegema, K., & Desai, A. (2014). A Bub1–Mad1 interaction targets the Mad1–Mad2 complex to unattached kinetochores to initiate the spindle checkpoint. *Journal of Cell Biology*, 204(5), 647-657.
- ³⁶ Cunha-Silva, S., & Conde, C. (2020). From the Nuclear Pore to the Fibrous Corona: A MAD Journey to Preserve Genome Stability. *BioEssays*, 42(11), 2000132.
- ³⁷ Vleugel, M., Tromer, E., Omerzu, M., Groenewold, V., Nijenhuis, W., Snel, B., & Kops, G. J. (2013). Arrayed BUB recruitment modules in the kinetochore scaffold KNL1 promote accurate chromosome segregation. *Journal of Cell Biology*, 203(6), 943-955.
- ³⁸ Zhang, G., Lischetti, T., & Nilsson, J. (2014). A minimal number of MELT repeats supports all the functions of KNL1 in chromosome segregation. *Journal of cell science*, 127(4), 871-884.
- ³⁹ Krenn, V., Overlack, K., Primorac, I., Van Gerwen, S., & Musacchio, A. (2014). KI motifs of human Knl1 enhance assembly of comprehensive spindle checkpoint complexes around MELT repeats. *Current Biology*, 24(1), 29-39.
- ⁴⁰ Kops, G. J., & Gassmann, R. (2020). Crowning the Kinetochore: The Fibrous Corona in Chromosome Segregation. *Trends in Cell Biology*.
- ⁴¹ Hara, M., & Fukagawa, T. (2020). Dynamics of kinetochore structure and its regulations during mitotic progression. *Cellular and Molecular Life Sciences*, 1-15.
- ⁴² Sacristan, C., Ahmad, M. U. D., Keller, J., Fermie, J., Groenewold, V., Tromer, E., ... & Musacchio, A. (2018). Dynamic kinetochore size regulation promotes microtubule capture and chromosome biorientation in mitosis. *Nature cell biology*, 20(7), 800-810.
- ⁴³ Craske, B., & Welburn, J. P. (2020). Leaving no-one behind: how CENP-E facilitates chromosome alignment. *Essays in Biochemistry*, EBC20190073.
- ⁴⁴ Pereira, C., Reis, R. M., Gama, J. B., Celestino, R., Cheerambathur, D. K., Carvalho, A. X., & Gassmann, R. (2018). Self-assembly of the RZZ complex into filaments drives kinetochore expansion in the absence of microtubule attachment. *Current Biology*, 28(21), 3408-3421.
- ⁴⁵ Cooke, C. A., Schaar, B., Yen, T. J., & Earnshaw, W. C. (1997). Localization of CENP-E in the fibrous corona and outer plate of mammalian kinetochores from prometaphase through anaphase. *Chromosoma*, 106(7), 446-455.
- ⁴⁶ Ciossani, G., Overlack, K., Petrovic, A., Koerner, C., Wohlgemuth, S., Maffini, S., & Musacchio, A. (2018). The kinetochore proteins CENP-E and CENP-F directly and specifically interact with distinct BUB mitotic checkpoint Ser/Thr kinases. *Journal of Biological Chemistry*, 293(26), 10084-10101.
- ⁴⁷ Caldas, G. V., Lynch, T. R., Anderson, R., Afreen, S., Varma, D., & DeLuca, J. G. (2015). The RZZ complex requires the N-terminus of KNL1 to mediate optimal Mad1 kinetochore localization in human cells. *Open biology*, 5(11), 150160.
- ⁴⁸ Gama, J. B., Pereira, C., Simões, P. A., Celestino, R., Reis, R. M., Barbosa, D. J., ... & Cheerambathur, D. K. (2017). Molecular mechanism of dynein recruitment to kinetochores by the Rod–Zw10–Zwilch complex and Spindly. *Journal of Cell Biology*, 216(4), 943-960.

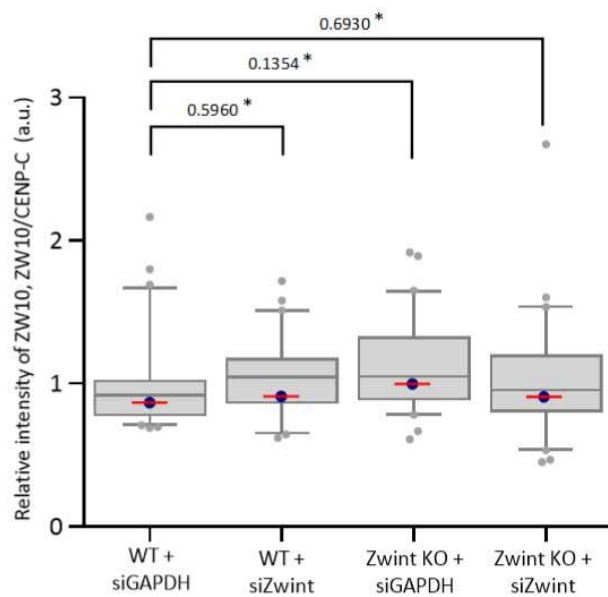
-
- ⁴⁹ Ji, W., Luo, Y., Ahmad, E., & Liu, S. T. (2018). Direct interactions of mitotic arrest deficient 1 (MAD1) domains with each other and MAD2 conformers are required for mitotic checkpoint signaling. *Journal of Biological Chemistry*, 293(2), 484-496.
- ⁵⁰ Chung, E., & Chen, R. H. (2002). Spindle checkpoint requires Mad1-bound and Mad1-free Mad2. *Molecular biology of the cell*, 13(5), 1501-1511.
- ⁵¹ De Antoni, A., Pearson, C. G., Cimini, D., Canman, J. C., Sala, V., Nezi, L., ... & Musacchio, A. (2005). The Mad1/Mad2 complex as a template for Mad2 activation in the spindle assembly checkpoint. *Current Biology*, 15(3), 214-225.
- ⁵² Luo, Y., Ahmad, E., & Liu, S. T. (2018). MAD1: kinetochore receptors and catalytic mechanisms. *Frontiers in cell and developmental biology*, 6, 51.
- ⁵³ Wang, H., Hu, X., Ding, X., Dou, Z., Yang, Z., Shaw, A. W., ... & Yao, X. (2004). Human Zwint-1 specifies localization of Zeste White 10 to kinetochores and is essential for mitotic checkpoint signaling. *Journal of Biological Chemistry*, 279(52), 54590-54598.
- ⁵⁴ Kops, G. J., Kim, Y., Weaver, B. A., Mao, Y., McLeod, I., Yates III, J. R., ... & Cleveland, D. W. (2005). ZW10 links mitotic checkpoint signaling to the structural kinetochore. *The Journal of cell biology*, 169(1), 49-60.
- ⁵⁵ Famulski, J. K., Vos, L., Sun, X., & Chan, G. (2008). Stable hZW10 kinetochore residency, mediated by hZwint-1 interaction, is essential for the mitotic checkpoint. *The Journal of cell biology*, 180(3), 507-520.
- ⁵⁶ Zhang, G., Lischetti, T., Hayward, D. G., & Nilsson, J. (2015). Distinct domains in Bub1 localize RZZ and BubR1 to kinetochores to regulate the checkpoint. *Nature communications*, 6(1), 1-14.
- ⁵⁷ Vos, L. J., Famulski, J. K., & Chan, G. K. (2011). hZwint-1 bridges the inner and outer kinetochore: identification of the kinetochore localization domain and the hZw10-interaction domain. *Biochemical Journal*, 436(1), 157-168.
- ⁵⁸ Lin, Y. T., Chen, Y., Wu, G., & Lee, W. H. (2006). Hec1 sequentially recruits Zwint-1 and ZW10 to kinetochores for faithful chromosome segregation and spindle checkpoint control. *Oncogene*, 25(52), 6901-6914.
- ⁵⁹ Kasuboski, J. M., Bader, J. R., Vaughan, P. S., Tauhata, S. B., Winding, M., Morrissey, M. A., ... & Hinchcliffe, E. H. (2011). Zwint-1 is a novel Aurora B substrate required for the assembly of a dynein-binding platform on kinetochores. *Molecular biology of the cell*, 22(18), 3318-3330.
- ⁶⁰ He, Y., Li, R., Gu, L., Deng, H., Zhao, Y., Guo, Y., ... & Wang, G. (2020). Anaphase-promoting complex/cyclosome-Cdc-20 promotes Zwint-1 degradation. *Cell Biochemistry and Function*.
- ⁶¹ Caldas, G. V., DeLuca, K. F., & DeLuca, J. G. (2013). KNL1 facilitates phosphorylation of outer kinetochore proteins by promoting Aurora B kinase activity. *Journal of Cell Biology*, 203(6), 957-969.
- ⁶² Varma, D., Wan, X., Cheerambathur, D., Gassmann, R., Suzuki, A., Lawrimore, J., ... & Salmon, E. D. (2013). Spindle assembly checkpoint proteins are positioned close to core microtubule attachment sites at kinetochores. *Journal of Cell Biology*, 202(5), 735-746.
- ⁶³ Goldberg, A. L. (1998). Proteasome inhibitors: valuable new tools for cell biologists. *Trends in cell biology*, 8(10), 397-403.

-
- ⁶⁴ Zieve, G. W., Turnbull, D., Mullins, J. M., & McIntosh, J. R. (1980). Production of large numbers of mitotic mammalian cells by use of the reversible microtubule inhibitor Nocodazole: Nocodazole accumulated mitotic cells. *Experimental cell research*, *126*(2), 397-405.
- ⁶⁵ Rueden, C. T., Schindelin, J., Hiner, M. C., DeZonia, B. E., Walter, A. E., Arena, E. T., & Eliceiri, K. W. (2017). ImageJ2: ImageJ for the next generation of scientific image data. *BMC bioinformatics*, *18*(1), 529.
- ⁶⁶ Potapova, T., & Gorbsky, G. J. (2017). The consequences of chromosome segregation errors in mitosis and meiosis. *Biology*, *6*(1), 12.
- ⁶⁷ Ying, H., Xu, Z., Chen, M., Zhou, S., Liang, X., & Cai, X. (2018). Overexpression of Zwint predicts poor prognosis and promotes the proliferation of hepatocellular carcinoma by regulating cell-cycle-related proteins. *OncoTargets and therapy*, *11*, 689.
- ⁶⁸ Wang, H. J., Wang, L., Lv, J., Fu, L. Q., Wang, Z., He, X. L., ... & Yu, L. L. (2017). Decreased expression of Zwint-1 is associated with poor prognosis in hepatocellular carcinoma. *International Journal of Clinical and Experimental Pathology*, *10*(10), 10406.
- ⁶⁹ Yang, X. Y., Wu, B., Ma, S. L., Yin, L., Wu, M. C., & Li, A. J. (2018). Decreased expression of ZWINT is associated with poor prognosis in patients with HCC after surgery. *Technology in cancer research & treatment*, *17*, 1533033818794190.
- ⁷⁰ Yuan, W., Xie, S., Wang, M., Pan, S., Huang, X., Xiong, M., ... & Shao, L. (2018). Bioinformatic analysis of prognostic value of ZW10 interacting protein in lung cancer. *OncoTargets and therapy*, *11*, 1683.
- ⁷¹ Kim, J. H., Youn, Y., Lee, J. C., Kim, J., & Hwang, J. H. (2020). Involvement of the NF- κ B signaling pathway in proliferation and invasion inhibited by Zwint-1 deficiency in Pancreatic Cancer Cells. *Journal of Cancer*, *11*(19), 5601.
- ⁷² Zhou, G., Shen, M., & Zhang, Z. (2020). ZW10 Binding Factor (ZWINT), a Direct Target of Mir-204, Predicts Poor Survival and Promotes Proliferation in Breast Cancer. *Medical Science Monitor: International Medical Journal of Experimental and Clinical Research*, *26*, e921659-1.
- ⁷³ Peng, F., Li, Q., Niu, S. Q., Shen, G. P., Luo, Y., Chen, M., & Bao, Y. (2019). ZWINT is the next potential target for lung cancer therapy. *Journal of cancer research and clinical oncology*, *145*(3), 661-673.
- ⁷⁴ Li, H. N., Zheng, W. H., Du, Y. Y., Wang, G., Dong, M. L., Yang, Z. F., & Li, X. R. (2020). ZW10 interacting kinetochore protein may serve as a prognostic biomarker for human breast cancer: An integrated bioinformatics analysis. *Oncology Letters*, *19*(3), 2163-2174.
- ⁷⁵ Yang, L., Han, N., Zhang, X., Zhou, Y., Chen, R., & Zhang, M. (2020). ZWINT: A potential therapeutic biomarker in patients with glioblastoma correlates with cell proliferation and invasion. *Oncology Reports*, *43*(6), 1831-1844.

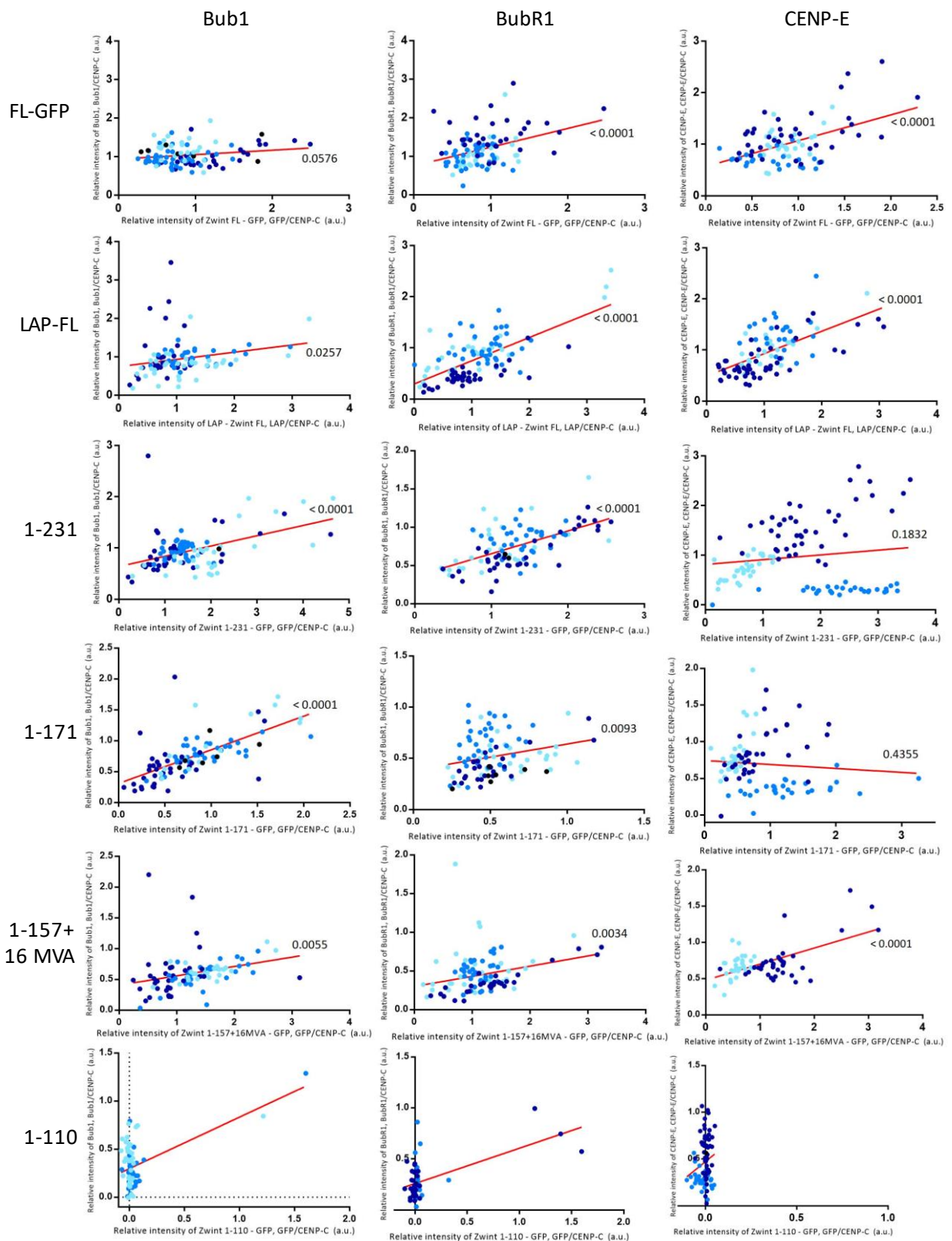
Supplemental figures



Supplemental figure 1: Quantification of kinetochore localization of BubR1 in MG132-treated cells.



Supplemental figure 2: Quantification of kinetochore localization of ZW10 in noco-treated cells.



Supplemental figure 3: Comparison between kinetochore localization of the protein of interest (respectively Bub1, BubR1, CENP-E, and localization of the Zint-1 rescue constructs. Dots represent kinetochore localization values of both parameters, and the colours represent repeated experiments. Regression line was calculated regarding the total population of datapoints for each protein.